THE CHAMP IN CLUSTER DETECTION: X-RAY VERSUS OPTICAL METHODS

Wayne A. Barkhouse and P.J. Green (Harvard-Smithsonian Center for Astrophysics), D. A. Perley (Cornell University), and the ChaMP Collobration

X-Ray Detection

Find clusters in archival Chandra data using the wavelet transform algorithm, and verify them by searching for the red sequence signature in a color-magnitude plot of their galaxies.

X-Ray Cluster Detection and ChaMP

Searching for clusters in X-ray observations affords many observations over optical searches, being immune to line-of-sight projection effects and more resistant to background effects: non-Galactic sources of extended X-ray emission is almost always associated with a galaxy cluster.

X-ray cluster surveys are slow and time-intensive. However, a wealth of data well-suited to this purpose is available in the Chandra archive: background regions of images of any small, high Galactic-latitude source are potential cluster search regions. The ChaMP (Chandra Multiwavelength Project) database – an extensive archive of Chandra fields and matching images at other wavelengths – is ideally suited for this purpose.

For our study, we used an extended source detection algorithm (described below) on 62 ChaMP pointings covering 5.826 square degrees. A histogram of exposure times is plotted in Figure 2.

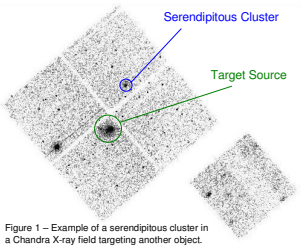

Figure 1 – Example of a serendipitous cluster in a Chandra X-ray field targeting another object.

Detection Algorithm

The ChaMP X-ray pipeline (Kim 2004) uses a wavelet transform algorithm to identify sources in X-ray count data. Most sources identified this way are point sources, and not cluster candidates, so the pipeline also contains an extended source detection algorithm, which fits each detected source with a circular Gaussian profile in the S band (0.3 - 2.5 keV), and compares the fitted width with the theoretical width of the Chandra PSF for the off-axis angle of the source. Sources significantly larger than this measure are flagged as extended, and analyzed visually.

In all, a total of 15 sources were flagged as extended were detected by this method. Added to this list were 6 sources manually flagged as extended during the Chandra visualization and verification (V&V) process, bringing the size of the candidate list to 21 sources.

All sources were observed visually in X-ray to eliminate clear non-cluster sources. Three sources were identified with an interacting galaxy system and excluded from the candidate list, and six were rejected as spurious detections, leaving 12 cluster candidates.

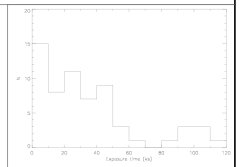

Figure 2 – Histogram of exposure times of Chanrda observations used in the X-ray cluster search.

Figure 3 – Color-magnitude diagrams in *g-i* vs. *i* of a confirmed cluster (a) and rejected cluster candidate (b). The diagram at bottom (c) demonstrates the technique of red-sequence estimation of *z*.

Red Sequence Verification

X-ray techniques are not immune to spurious detections, especially for the faintest clusters, which may generate only a few extra counts. Optical verification is therefore important to ensure accuracy of the results.

While sometimes a clear optical overdensity of galaxies is evident visually, a more reliable way to confirm a cluster is by observation of a "red sequence" – a population of early-type galaxies, which in a single cluster tend to have similar (reddish) color. A plot of color versus magnitude in the region of a suspected cluster can determine its status based on the presence or absence of an observed horizontal bar (Figure 3a) for clusters of $z < 0.6$.

The ChaMP has obtained deep optical imaging using the NOAO 4meter telescopes and MOSAIC imagers at KPNO and CTIO. ChaMP imaging in 3 bands (SDSS *g'*, *r'*, and *i'*) in the 36' MOSAIC field of view obtains typical (5•) depths of 24.5mag. Color-magnitude diagrams in *g-i* versus *i* were used in this way to identify the red sequence and evaluate the status in each possible cluster.

ChaMP optical photometry was available for 8 of the 12 candidate clusters. Of these, two were known clusters, leaving 6 remaining candidates. Of these, all but two appear on account of either their red sequences or visual analysis of the X-ray and optical images to be galaxy clusters.

Galaxies near the center of several of the candidate clusters were observed spectroscopically to determine the redshifts of these objects (see Results.) In addition, red-sequence galaxies exhibit a useful spectral "break" near 4000 Å, causing their photometric color to evolve sharply with redshift. This allows them to serve as estimators of the cluster's redshift independent of spectroscopic observations. We used the program HyperZ (Bolzonella et al. 2000) to calculate the theoretical evolution of a standard M* elliptical galaxy with redshift. The point where the observed red sequence intersected with the resulting "track" was taken as the photometric redshift.

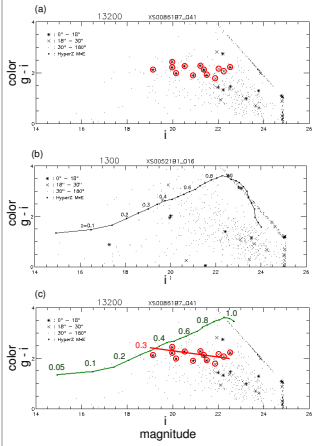

New Cluster Detections

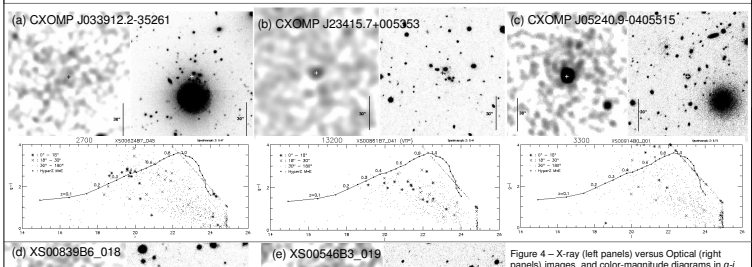

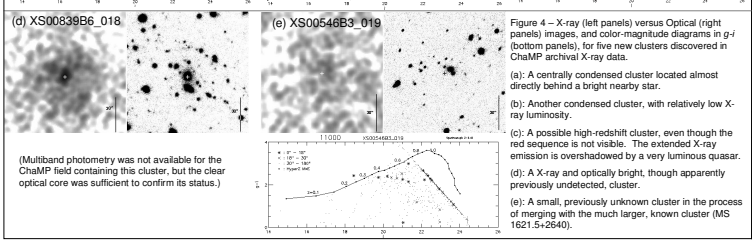

(Multiband photometry was not available for the ChaMP field containing this cluster, but the clear optical core was sufficient to confirm its status.)

Figure 4 – X-ray (left panels) versus Optical (right panels) images, and color-magnitude diagrams in *g-i* (bottom panels), for five new clusters discovered in ChaMP archival X-ray data.

(a): A centrally condensed cluster located almost directly behind a bright nearby star.

(b): Another condensed cluster, with relatively low X-ray luminosity.

(c): A possible high-redshift cluster, even though the red sequence is not visible. The extended X-ray emission is overshadowed by a very luminous quasar.

(d): A X-ray and optically bright, though apparently previously undetected, cluster.

(e): A small, previously unknown cluster in the process of merging with the much larger, known cluster (MS 1621.5+2640).

Optical Detection

Find clusters in deep optical images using the Voronoi Tessellation and Percolation algorithm on filtered photometric catalogs.

VTP: Voronoi Tessellation and Percolation

Voronoi Tesselation and Percolation (Ebeling & Wiedemann 1993) is a relatively recent algorithm designed for efficient, scale- and morphology-independent source detection in coordinate data. Tessellation assigns every point in the field to a polygonal cell consisting of the area of the field closer to that point than any other (Figure 5). The smallest cells are then percolated outward, with adjacent cells being added to the region until the sizes of the newly added cells drop to the background level. These detections are assigned a confidence level based on their cell size distribution and either rejected (if the density is too low) or accepted and output (along with an estimate the cluster center and radius) as candidate clusters. The VTP algorithm used here was the Voronoi Galaxy Cluster Finter (VGCF, Ramella et. al. 2002).

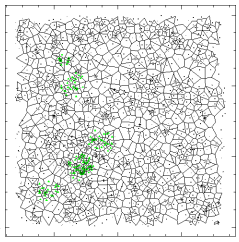

Figure 5 – Example of a VTP-tessellated optical field. Candidate clusters are marked in green.

Color-Magnitude Filter Binning

Because of the dense galaxy background in deep optical images, purely random overdensities of unrelated galaxies are relatively common. In addition, the filamentary nature of large-scale cosmological structure often causes cluster-like projections along the line of sight. As a result, optical searches are highly vulnerable to spurious detections, and real clusters may be missed due to insufficient contrast with the background.

The effective background can, however, be reduced via color-magnitude filtering that examines individual color-magnitude slices appropriate for red-sequence elliptical galaxies in bins determined by their theoretical redshift-evolution. These filtered data sets are given to VTP (above), which generates a list of candidate clusters for each filter. These lists are then synthesized into a single master list, taking into account those objects which are located in multiple bins.

With appropriate choice of photometric filters, the number of spurious detections in an overdensity search should be reduced, and the sensitivity to real clusters increased, compared to runs on unfiltered catalog data.

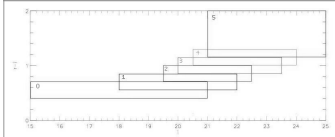

Figure 6 – The six color-magnitude bins used to filter photometric data in preparation for VTP. The bins were chosen based on the theoretical evolution of an M* elliptical galaxy with redshift.

Performance on Known Clusters

In advance of the full run on the entire ChaMP database, the fields containing those likely clusters detected in X-ray (left), and some other fields containing known clusters, were used as test fields for the algorithm.

• The cluster in Figure 4e was successfully found; the VTP-generated red sequence is presented in Figure 7a. This VTP red sequence is less visible than the *g-i* red sequence in Figure 4b due to VTP's poor centering accuracy, but is still reasonably clear.

• The cluster in Figure 4b and the known cluster with which it appears to be merging were successfully detected, though as a single object.

• The clusters in Figure 4a and 4c were not found. It is likely that contamination from the nearby bright star contributed to the fact that 4a was missed, and 4c does not even have a visible red sequence.

• VTP successfully found the bright nearby optical cluster Abell 0447, but not a known X-ray - selected cluster at redshift 0.7.

Unsurprisingly, VTP appears to be best-suited to finding clusters with relatively dense optical cores at redshifts less than 0.6.

Detections of New Clusters

A complete scan of all available ChaMP optical fields was completed on January 1. Most of these results have yet to be analyzed, but a preliminary assessment of the ability of VTP to detect new clusters is still possible based on analysis of the background regions of the optical fields used to assess the performance of VTP in detecting known clusters.

An example of a possible new cluster is presented in Figure 6b. This object is detected independently in four different filter bands and a red sequence appears to be visible in an appropriate location for a redshift of about 0.4. Several similar-looking plots were observed in the other fields (averaging between zero and two such candidates per 0.75" x 0.75" field).

Color-magnitude binning increases sensitivity, but may not reduce spurious detections: the average number of detections per field is about 15-20, most of which appear to be spurious. Some of the spurious detections are easily excluded by visual analysis of the plots (Figure 6c). Others may be examples of large-scale structure (projected filaments), a problem endemic to optical cluster selection. Simulations are now underway to estimate the completeness and sensitivity of our optical cluster detection.

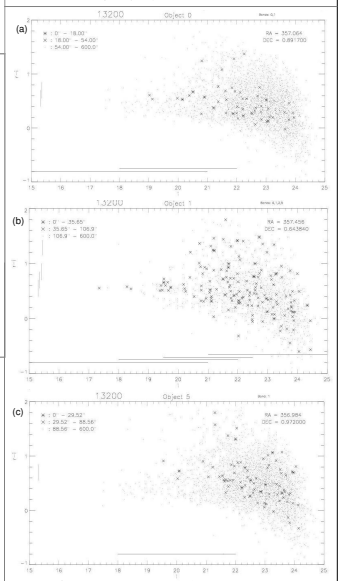

Figure 7 – Color-magnitude plots (*r-i* vs *i*) for three detected objects in a VTP scan. Large symbols indicate objects within the VTP-derived cluster regions; small dots are background objects (within 10')

(a): A known cluster found in ChaMP X-ray fields (see Figure 4b).

(b): A possible new cluster detected by filtered VTP.

(c): Example of a false VTP detection. In general such spurious detections can be eliminated as clusters visually, but ambiguous cases do arise.

Summary

Using automatic and manual methods, we search 62 Chandra observations retrieved from archival data in ChaMP for extended sources. We use visual inspection and red-sequence analysis to eliminate spurious detections and non-cluster sources, finding five new probable clusters and one additional cluster candidate.

With our deep multiband NOAO 4-meter imaging we also investigate Voronoi Tessellation and Percolation (VTP) with red sequence-based color filtration as a potential cluster finding tool. Filtered VTP detects most known X-ray selected clusters and several likely new clusters. Detailed simulations, and comparison to the X-ray cluster detections in the same deep ChaMP fields offers a unique opportunity to contrast X-ray and optical detection methods for clusters at both high redshift and low luminosity, over the wide (14 deg²) ChaMP sky area.

Acknowledgements

The Chandra Multiwavelength Project (ChaMP) is supported by NASA under CXC archival research grants. Optical images were obtained at the KPNO and CTIO 4meter telescopes, through the National Optical Astronomy Observatory (NOAO), operated by the Association of Universities for Research in Astronomy, Inc. (AURA) under cooperative agreement with the National Science Foundation.

References

Bahcall, N. A., Cen, R. 1993, Ap. J., 407, L49
Bertin, E., Arnouts, S. 1996, A&AS, 117, 393
Borgani, S., Rosati, P., Tozzi, P., Stanford, S. A., Eisenhardt, P. R., Lidman, C., Holden, B., Della Ceca, R., Norman, C., Squires, G. 2001, Ap. J., 561, 13
Bolzonella, M., Miralles, J.-M., Pelló, R. 2000, !aap, 363, 476
Boschin, W. 2003, A. & Ap., preprint
Collins, C. A., Guzzo, L., Bohringer, H., Schuecker, P., Chincarini, G., Cruddace, R., De Grandi, S., MacGillivray, H. T., et al. 2000, Mon. Not. R. Ast. Soc., 319, 939
Dressler, A., Oemler, A. Jr., Couch, W. J., Smail, I., Ellis, R. S., Barger, A., Butcher, H., Poggianti, B. M., Sharples, R. M. 1997, Ap. J., 490, 577
Ebeling, H., Wiedemann, G. 1993, Phys. Rev. E, 47, 704
Eisenstein, D. J., James, A., Gunn, J. E., Szalay, A. S., Connolly, A. J., Nichol. R. C., Bahcall, N. A., Bernardi, M., et al. 2001, A. J., 122, 2267
Ellingson, E., Lin, H., Yee, H. K. C., Carlberg, R. G. 2001, Ap. J., 547, 609
Ettori, S., Tozzi, P., Rosati, P. 2003, A. & Ap., 398, 879
Freeman, P. E., Kashyap, V., Rosner, R., Lamb, D. Q. Others. Ap. J.s, 138, 185
Fukujita, M., Shimasaku, K., Ichikawa, T. 1995, P. A. S. P., 107, 945
Gladders, M. D., Yee, H. K. C. 2000, A. J., 120, 2148
Gonzalez, A. H., Zaritsky, D., Simard, L., Clowe, D., White, S. D. M. 2002, Ap. J., 579, 577
Girardi, M., Borgani, S., Giuricin, G., Mardirossian, F., Mezzetti, M. 1998, Ap. J., 506, 45
Green, P., J., Silverman, J. D., Cameron, R. A., Kim, D. W., Wilkes, B. J., Barkhouse, W.A., LaCluyze, A., Morris, D., et al. 2004, in press.
Kim, D.-W., Cameron, R. A., Drake, J. J., Evans, N., Freeman, P., Gaetz, T. J., Ghosh, H., Green, P. J., et al. 2004, Submitted.
Kelson, D. D., van Dokkum, P. G., Franx, M., Illingworth, G. D., Fabricant, D. 1997, Ap. J., 478, L13
Mauskopf, P. D., Ade, P. A. R., Allen, S. W., Church, S. E., Edge, A. C., Ganga, K. M., Holzapfel, W. L., Lange, A. E., et al. Ap. J., 536, 505.
Nichol, R. C., Collins, C. A., Guzzo, L., Lumsden, S. L. 1992, Mon. Not. R. Ast. Soc., 255, 21
Perlam, E. S., Horner, D. J., Jones, L. R., Scharf, C. A., Ebeling, H., Wegner, G., Malkan, M. 2002, Ap. J.s, 140, 265
Ramella, M., Boschin, W., Fadda, D., Nonino, M. 2002, A. & Ap., 368, 776
Rosati, P., Borgani, S., Norman, S. 2002, A. R. A. A., 40, 539
Schuecker, P., Bohringer, H., Guzzo, L., Collins, C. A., Neumann, D. M., Schindler, S., Voges, W., DeGrandi, S., et al., Shaver, P., 2001, A. & A. P., 368, 86
van Dokkum, P. G., Franx, M. 2001, Ap. J., 553, 90
Vikhlinin, A., VanSpeybroeck, L., Markevitch, M., Forman, W. R., Grego, L. 2002, Ap. J., 578, L107